NRIAG Journal of Astronomy and Geophysics (2015) 4, 100–105

National Research Institute of Astronomy and Geophysics

NRIAG Journal of Astronomy and Geophysics

www.elsevier.com/locate/nrjag

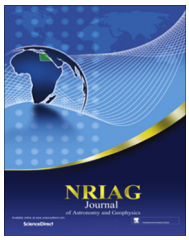

On the arrival times of halo Coronal Mass Ejections in the vicinity of the Earth

Nishant Mittal *, **Udit Narain**

Astrophysics Research Group, Dept. of Physics, Meerut College, Meerut 250002, India

Received 31 August 2014; revised 2 March 2015; accepted 4 May 2015
Available online 26 June 2015

KEYWORDS

Sun;
Coronal Mass Ejections;
ICMEs;
Arrival time;
Solar flare

Abstract It is well known that the arrival times of Coronal Mass Ejections (CMEs) in the vicinity of the Earth play an important role for solar terrestrial environment. It is necessary to predict the CMEs arrival time at 1 AU, for the better forecasting of space weather. Here, using LASCO halo CMEs data of 248 events observed during time period 1996–2007, we have tried to predict the arrival times as accurately as possible of full halo CMEs only. We have also studied arrival time of halo CMEs associated with type II radio bursts and X-class soft X-ray bursts, separately. In this paper we discussed about location and speed of Earth directed CMEs. The results obtained in the present investigation are discussed in the light recent scenario of CMEs understanding.

1. Introduction

It is now well-known that space weather is significantly controlled by Coronal Mass Ejections (CMEs) which can affect our Earth environment in many ways (Gopalswamy, 2006; Gopalswamy et al., 2007; Iyer et al., 2006; Srivastava, 2006; Dumbovic et al., 2015). CMEs originating close to the central meridian of the Sun directed towards the Earth are the most geoeffective one with the biasing of source region to the western hemisphere. For space weather forecasts (geomagnetic storms, hazards to humans in space, effects on satellites, radio communication, GPS satellite errors, geomagnetic induced current, aurora) it is very important to know when a solar disturbance would reach the Earth (Srivastava and Venkatakrishnan, 2004; Gopalswamy et al., 2008). CMEs are dynamically expelled and driven by the coronal magnetic fields which decrease during their passage through the interplanetary space where some other processes (such as magnetic flux, current sheath, shocks) may accelerate them. These CMEs interaction with the ambient solar wind may provide the necessary drag for acceleration or de-acceleration of CMEs depending on their speeds (see e.g., Michalek et al., 2004; Manoharan et al., 2004 and references therein).

On combining CME observations made by SOHO/LASCO and interplanetary CMEs (ICMEs) (main causes for geomagnetic storms) measurements near the Earth, Gopalswamy et al. (2001), developed an empirical model to predict the arrival time of CMEs at 1-AU. They postulated that CMEs undergo an effective acceleration mechanism due to

* Corresponding author.
E-mail address: nishantphysics@yahoo.com (N. Mittal).
Peer review under responsibility of National Research Institute of Astronomy and Geophysics.

http://dx.doi.org/10.1016/j.nrjag.2015.05.001
2090-9977

interaction with the solar wind. This effective acceleration was assumed to be constant over the Sun–Earth distance and was defined as the difference between the initial (u) and final (v) speeds divided by the time (t) taken by a given CME to reach the Earth. They found a definite correlation between the effective acceleration (a) and initial speed (u) which is given below:

$$a_1 = 1.41 - 0.0035u \quad (1)$$

They improved their model by taking into account the projection effects which now becomes,

$$a_2 = 2.193 - 0.0054u \quad (2)$$

Here a_1, a_2 and u are in units of km/s^2 and km/s, respectively.

These relations can be used in the kinematics equation,

$$S = ut + \frac{1}{2}at^2 \quad (3)$$

where S is the distance travelled by the CME to predict arrival time at 1-AU. Their model involves only one free parameter, "namely, the initial speed of CMEs". With some modifications, they were able to predict the travel time within an error of 10.7 h.

Michalek et al. (2004) used a better method to obtain the space speed (the speed with which the CME spreads in the space) of CMEs which minimizes the projection effects for full halo CMEs. The plane of the sky values can deviate from the real radial speed of the CME front, depending on the actual direction of the motion. They consider only full halo (FH) CMEs (width 360°). Their sample includes CMEs of wider range of initial velocities. To improve prediction, they introduce the effective acceleration from two groups of CMEs which do not have acceleration cessation at any place between the Sun and Earth. Further the acceleration cessation distance is dependent on the initial velocity of a given event.

The new linear relation connecting acceleration with initial velocity of CMEs is

$$a_3 = 4.11 - 0.0063u \quad (4)$$

Clearly the coefficients of this relation differ from those of Eqs. (1) and (2) because the relation (4) depends on a data set which includes several fast CMEs.

Another linear relation which is based on the assumption that CMEs do not stop accelerating at any place between the Sun and Earth, reads as follows:

$$a_4 = 3.35 - 0.0074u \quad (5)$$

But the relation

$$a_5 = 2.99 - 0.0067u \quad (6)$$

leads to better travel times when uncorrected initial velocities "u" are used (Michalek et al., 2004).

Using this method they were able to predict the arrival times of HCMEs with an average error of 8.7 h and 11.2 h for space and projected initial velocities, respectively. They conclude that each population of CMEs may need a separate acceleration profile for an accurate prediction in which the average effective acceleration depends only on the initial velocity.

Owens and Cargill (2004) analyse the causes of errors in arrival times of CMEs at 1-AU in the models, namely constant acceleration/deceleration model of Gopalswamy et al. (2000), cessation of acceleration before 1-AU model of Gopalswamy et al. (2001) and aerodynamic model of Vrsnak and Gopalswamy (2002). They discuss possible sources of error and possibilities of improvements.

Taking above approaches into consideration, we consider it worthwhile to determine the arrival times of CMEs at Earth taking a larger database. In the next section (Section 2) we present data set used, and in Section 3 we present our model and obtained results. Section 4 describes about location of HCMEs and Section 5 describes about the speed of HCMEs. In Section 6 we discuss our result. The last section (Section 7) contains our conclusions.

2. Data

The data used in this study include only full Halo CMEs that occurred between 1996 and 2007 and hit the Earth. We use LASCO data for studying the solar origins of the CMEs. The data for CMEs have been taken from the catalogue maintained by the Centre for Solar Physics and Space Weather (CSPSW) (http://cdaw.gsfc.nasa.gov/CME_list) and other data were taken from Gopalswamy et al. (2001), Michalek et al. (2004), Manoharan et al. (2004) and Gopalswamy et al. (2007). The Large Angle Spectroscopic Coronagraph (LASCO) imaging instrument on board SOHO (Brueckner et al., 1995) currently has two functioning coronagraphs, C2 which has a field of view (FOV) of 1.5–6 R_S and a cadence of around 30 min, and C3 with a FOV of 3.7–30 R_S and cadence of around 50 min. The C1 telescope that can observe CMEs closer to the Sun was disabled in June 1998. It may be remarked that there is a data gap during the period July–September 1998, because during this period SOHO satellite became inoperational (Gopalswamy et al., 2009; Mittal et al., 2009b).

Since the major cause of the space weather disturbances is Earth directed full HCMEs, so we have taken only Earth directed full HCMEs in our study. All the Earth directed HCMEs have been taken from Gopalswamy et al. (2007).

For each event the catalogue contains height-time plots, plane of sky speeds and the corresponding accelerations. The CME speed is determined from both the linear and the quadratic fits to the height-time measurements. In our study we analyse the linear (constant speed) fit which is preferable for 90% of the CMEs (Mittal et al., 2009a).

The definition of full or partial halo is based on the azimuthal extent of CMEs in the LASCO field of view (Webb et al., 2000). The data of type II radio burst (frequency range 1–14 MHz) are taken from WIND/WAVES catalogue and the data of solar flares ($>$X1) are taken from GOES.

The observed arrival time is marked by the time at which the D_{ST} index becomes minimum.

3. Model and results

In this section we have discussed arrival time of HCMEs. We have grouped the halo CMEs in different categories. In first we have taken all the Earth directed HCMEs and created three groups. Firstly we have studied all the Earth directed HCMEs and than CMEs having speed >500 km/s and CMEs having speed <500 km/s. We have also studied that whether HCMEs are associated with type II radio burst, X-class flares or with both radio bursts and X-class solar flares

than which one is better predicted arrival time of HCMEs to avoid space weather effects.

3.1. Arrival time of HCMEs in the vicinity of the Earth

We have selected 248 events and attempted a linear fit between arrival times (T_1) and corresponding initial velocities (u) and obtained the following relation:

$$T_1 = -0.0114u + 76.744 \quad (7)$$

where arrival time T_1 is in hours and the initial speed u is in km/s. In this case u ranges from 87 to 3387 km/s, thus all the 248 events have been taken into account.

Another linear relation between arrival times and initial velocities was obtained for 210 events whose initial velocities were greater than 500 km/s and this relation reads as follows:

$$T_2 = -0.01234u + 78.373 \quad (8)$$

We tried to obtain a linear fit for CMEs having initial velocities less than 500 km/s. The resulting relation is

$$T_3 = -0.0604u + 92.791 \quad (9)$$

This formula is based on 38 CME events.

The arrival times calculated using Eqs. (7)–(9) are exhibited in Figs. 1–3 as a function of initial velocities. The solid line represents the calculated arrival times using Eqs. (7)–(9). The dotted lines correspond to errors of ±10 h. The original arrival times are exhibited by different symbols in these figures.

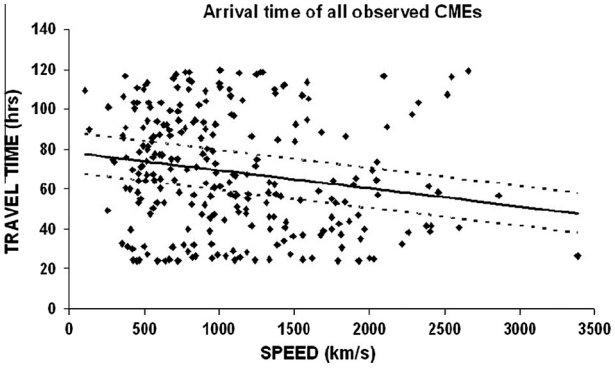

Fig. 1 A representative prediction solid line curve of HCME arrival time with the ±10 h boundaries is given by dotted lines. The diamonds denote the observed arrival times of 248 CMEs.

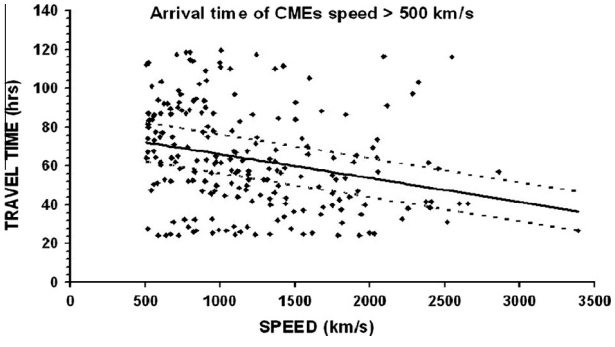

Fig. 2 A representative prediction solid line curve of HCME arrival time with the ±10 h boundaries is given by dotted lines. The diamonds denote the observed arrival times of 210 CMEs (speed > 500 km/s).

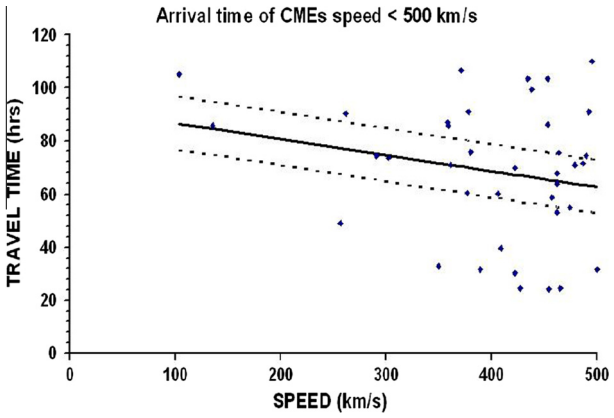

Fig. 3 A representative prediction solid line curve of HCME arrival time with the ±10 h boundaries is given by dotted lines. The diamonds denote the observed arrival times of 38 CMEs (speed < 500 km/s).

3.2. Arrival time of HCMEs associated with radio bursts in the vicinity of the Earth

We have selected 142 HCME events, which are associated with type II radio burst.

We attempted a linear fit between arrival times (T_4) and corresponding initial velocities (u) and obtained the following relation:

$$T_4 = -0.0077u + 76.374 \quad (10)$$

3.3. Arrival time of HCMEs associated with radio bursts and X-class solar flares in the vicinity of the Earth

We have selected 50 HCME events, which are associated with type II radio burst and X-class flares.

We tried to obtain a linear fit for HCMEs associated with radio bursts (1–14 MHz) and X-class solar flares (>X1) for the better prediction of arrival time of Earth directed HCMEs. The resulting relation is

$$T_5 = -0.0049u + 70.623 \quad (11)$$

3.4. Arrival time of HCMEs associated with X-class solar flares in the vicinity of the Earth

We have selected 58 HCME events, which are associated with X-class flares only.

$$T_6 = -0.00223u + 64.994 \quad (12)$$

4. Location of Earth directed HCMEs

Fig. 7 shows the distributions of source latitude and longitude of HCMEs. In Fig. 7 we have plotted solar disc locations of Earth directed HCMEs on x-axis as an east (−90° to 0°) to west (0–90°) longitude in degree and on y-axis as a south

(−90° to 0°) – north (0–90°) latitude in degree. The majority of the events originated within ±35° of the central meridian and ±30° of the equator. There appears to be no hemispherical preference in halo CMEs that reach the Earth, as reported by Cane et al. (2000) and Zhang et al. (2003).

5. Speed distribution of halo Coronal Mass Ejections

The histogram of distribution of speeds of 248 HCMEs during the period 1996–2007 is exhibited in Fig. 8. The CME speed listed in the LASCO CME catalogue is measured from the height time measurements projected in the sky plane. So all the measured parameters will suffer from projection effects; no attempt had been made to correct the projection effects. The average and median speeds of these HCMEs are found to be 1081 km/s and 951 km/s, respectively. Figure shows the speed of HCMEs varying from 200 km/s to more than 2500 km/s. Peak of the histogram occurs at 600 km/s.

6. Discussion

In their study Gopalswamy et al. (2000) study the 28 IP (interplanetary) events associated with CMEs and give an empirical model which works much better for fast CMEs compared to slow CMEs. In 2001, Gopalswamy et al. again describe an empirical model to predict the arrival time of CMEs at 1 AU by the selection of 47 ICME events. Their model predicts the arrival time with the error 15.4–10.7 h. This model is also in good agreement with high speed CMEs. In 2004, Michaek et al. studied the arrival time of Halo CMEs for 83 events. In their study Michalek et al. (2004) predicted the arrival time of HCMEs with an average error of 8.7 and 11.2 h for space and projected initial velocities, respectively. Our main aim has been to predict the arrival times of HCMEs in the vicinity of the Earth as correctly as possible. So we have grouped all the HCMEs into different categories to predict the better arrival time of HCMEs.

Fig. 1 exhibits arrival times (in h) of CMEs (thick line) calculated on the basis of Eq. (7) as a function their initial speed (in km/s) and the solid diamond symbols are observed arrival times (in h). The upper dotted line stands for an error of +10 h whereas the lower dotted line exhibits an error of −10 h. It is clear that discrepancies between observed and calculated times are quite significant. Thus the relation (7) needs modification.

In Fig. 2 we exhibit arrival times of 210 CMEs whose initial speeds are larger than 500 km/s using Eq. (8). In this figure the diamonds represents the observed arrival times.

Fig. 3 shows the distribution of arrival times of slow CMEs (speed < 500 km/s) using Eq. (9) with their initial speeds. The observed arrival times are shown by diamonds for all 38 events. Here the larger errors are more frequent although the data set was small. Thus the relation (9) also needs improvement.

Whereas Fig. 4 exhibits the distribution of arrival times for HCMEs associated with radio bursts, Fig. 5 shows the distribution of arrival times for HCMEs associated with radio bursts and X-class flares and Fig. 6 shows the distribution of arrival times for HCMEs associated with X-class flares.

Table 1 compares arrival times at different CME speeds as obtained from Eqs. (7), (10)–(12).

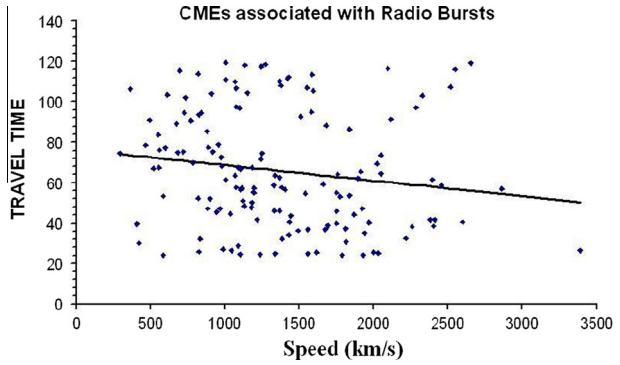

Fig. 4 A representative prediction solid line curve of HCME associated with type II radio burst arrival time. The diamonds denote the observed arrival times of 142 HCMEs associated with type II radio burst.

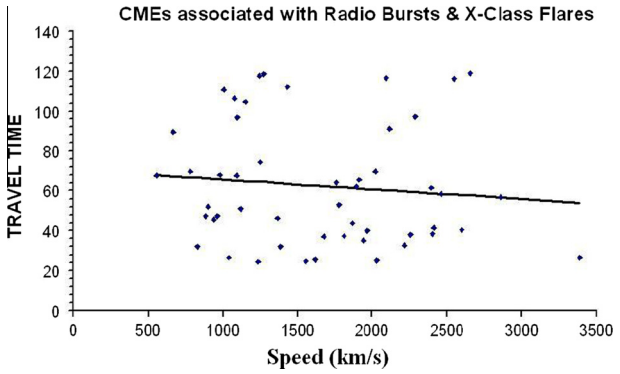

Fig. 5 A representative prediction solid line curve of HCME associated with type II radio burst and X-class flares arrival time. The diamonds denote the observed arrival times of 50 HCMEs associated with type II radio burst and X-class flares.

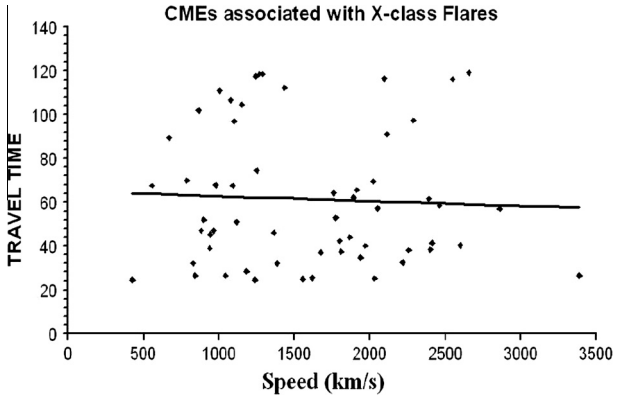

Fig. 6 A representative prediction solid line curve of HCME associated with X-class flares arrival time. The diamonds denotes the observed arrival times of 58 HCMEs associated with X-class flares.

Fig. 7 shows that the Earth directed HCMEs lies in the latitudinal range ±30° i.e. their distribution is symmetrical.

Fig. 8 shows speed distribution for all Earth directed HCMEs, which lies in the range 104–3387 km/s. It is clear

Table 1 Comparison between arrival times at different speeds obtained for different events.

Events	Arrival time (in h)						
	500 km/s	1000 km/s	1500 km/s	2000 km/s	2500 km/s	3000 km/s	3500 km/s
HCMEs	71.04	65.34	59.64	53.94	48.24	42.54	36.84
HCMEs and type II Radio burst	72.52	68.67	64.82	60.97	57.12	53.27	49.42
HCMEs and type II Radio burst and X-class flares	68.17	65.72	63.27	60.82	58.37	55.92	53.47
HCMEs and X-class flares	63.88	62.76	61.65	60.53	59.42	58.3	57.2

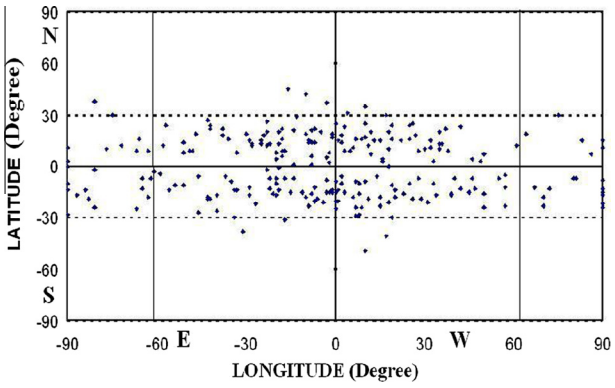

Fig. 7 Latitude and longitude distribution of Earth directed HCMEs.

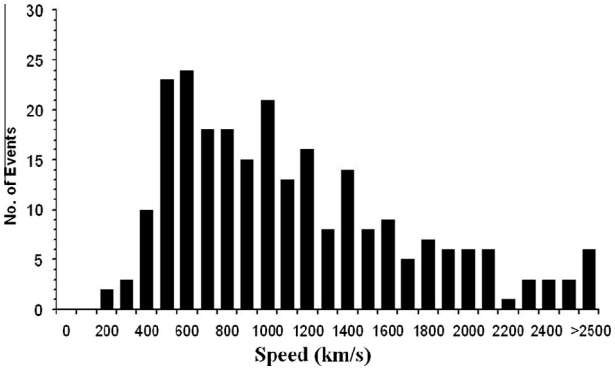

Fig. 8 Histogram showing the speed distribution of 248 HCMEs.

from Figs. 7 and 8 the direction of CMEs towards Earth depends on their location on Sun, not on their speed.

Owens and Cargill (2004) have discussed the predictions of the arrival times of CMEs at 1-AU. They found that projection effects are not the major cause of the error in the arrival times. They also find that there is a weak trend towards early arrival for stronger magnetic field strength ICMEs. Further the late arriving ICMEs have both thicker sheath regions and lower magnetic field intensities. They conjecture that the primary cause of error in arrival times is most likely a geometrical effect which can arise for two reasons. First, from a single in situ observation of ICMEs, one does not know which part of the event one is sampling. Since an ICME is a curved 3-D structure the measured arrival time will depend on which part of the ICME is being sampled. Second, ICMEs become deformed in the interplanetary medium, with an elongation taking place in a direction perpendicular to the principal direction of the motion. Hence STEREO mission observations can give a better determination of the velocity vector of the CME at the Sun. In their study, Mishra and Srivastava (2013) studied kinematics of eight CMEs by exploiting the STEREO COR2 and HI observations. The speed of events selected by them ranges from low (335 km s^{-1}) to high (870 km s^{-1}) in the COR2 field of view. They calculated the arrival time using these data with error 3–9 h.

7. Conclusions

The main results of an investigation carried out in previous section are as follows:

1. The observed travel time is fairly correlated with various speeds of CMEs.
2. The calculated travel time is excellently correlated with various speeds of CMEs.
3. The direction of CMEs towards Earth does not depend on associated activities.
4. The 70% of Earth directed HCMEs are located within $\pm 30°$ of solar disc centre.
5. Speed of HCMEs varies from 200 km/s to more than 2500 km/s.

Acknowledgements

The authors would like to thank for the excellent LASCO-CME catalogue, which includes supportive data. Authors are also thankful to WIND/WAVES and GOES for providing relative data.

References

Brueckner, G.E. et al, 1995. The large angle spectroscopic coronagraph (LASCO). Sol. Phys. 162, 357.

Cane, H.V., Richardson, I.G., St. Cyr, O.C., 2000. Coronal mass ejections, interplanetary ejecta and geomagnetic storms. Geophys. Res. Lett. 27, 3591.

Dumbovic, M., Devos, A., Vrsnak, B., Sudar, D., Rodriguez, L., Ruzdjak, D., Leer, K., Vennerstrøm, S., Veronig, A., 2015. Geoeffectiveness of coronal mass ejections in the SOHO era. Sol. Phys. 290 (2), 579.

Gopalswamy, N., Lara, A., Lepping, R.P., Kaiser, M.L., Berdichevsky, D., St. Cyr, O.C., 2000. Interplanetary acceleration of coronal mass ejections. Geophys. Res. Lett. 27, 145.

Gopalswamy, N., Lara, A., Yashiro, S., Kaiser, M.L., Howard, R.A., 2001. Predicting the 1-AU arrival times of coronal mass ejections. J. Geophys. Res. 106 (A12), 29207.

Gopalswamy, N., 2006. Coronal mass ejections of cycle 23. J. Astrophys. Astron. 27, 243.

Gopalswamy, N., Yashiro, S., Akiyama, S., 2007. Geoeffectiveness of halo coronal mass ejections. JGR Space Phys. 112 (A6), A06112.

Gopalswamy, N., Akiyama, S., Yashiro, S., Michalek, G., Lepping, R.P., 2008. Solar sources and geospace consequences of interplanetary magnetic clouds observed during solar cycle 23. J. Atmos. Sol.-Terrestrial Phys. 70, 245.

Gopalswamy, N., Yashiro, S., Michalek, G., Stenborg, G., Vourlidas, A., Freeland, S., Howard, R., 2009. The SOHO/LASCO CME catalog. Earth, Moon, Planets 104 (1), 295.

Iyer, K.N., Jadav, R.M., Jadeja, A.K., Manoharan, P.K., Sharma, S., Vats, H.O., 2006. Space weather effects of coronal mass ejection. J. Astrophys. Astron. 27, 219.

Manoharan, P.K., Gopalswamy, N., Yashiro, S., Lara, A., Michalek, G., Howard, R.A., 2004. Influence of coronal mass ejection interaction on propagation of interplanetary shocks. J. Geophys. Res. 109, A06109.

Michalek, G., Gopalswamy, N., Lara, A., Manoharan, P.K., 2004. Arrival time of halo coronal mass ejections in the vicinity of the Earth. A&A 423, 729.

Mittal, N., Sharma, J., Tomar, V., Narain, U., 2009a. On distribution of CMEs speed in solar cycle 23. Planet. Space Sci. 57/1, 53.

Mittal, N., Pandey, K., Narain, U., Sharma, S.S., 2009b. On properties of narrow CMEs observed with SOHO/LASCO. Astrophys. Space Sci. 323 (2), 135.

Mishra, W., Srivastava, N., 2013. Estimating the arrival time of earth-directed coronal mass ejections at in situ spacecraft using COR and HI observations from STEREO. ApJ 772, 70.

Owens, M., Cargill, P., 2004. Predictions of the arrival time of Coronal Mass Ejections at 1AU: an analysis of the causes of errors. Ann. Geophys. 22, 661.

Srivastava, N., Venkatakrishnan, P., 2004. Solar and interplanetary sources of major geomagnetic storms during 1996–2002. J. Geophys. Res. 109, A10103.

Srivastava, N., 2006. The challenge of predicting the occurrence of intense storms. J. Astrophys. Astron. 27, 237.

Vrsnak, B., Gopalswamy, N., 2002. Influence of the aerodynamic drag on the motion of interplanetary ejecta. J. Geophys. Res. 107 (A2), SSH 2-1.

Webb, D.F., Cliver, E.W., Crooker, N.U., St. Cry, O.C., Thompson, B.J., 2000. Relationship of halo coronal mass ejections, magnetic clouds, and magnetic storms. J. Geophys. Res. 105 (A4), 7491.

Zhang, J., Dere, K.P., Howard, R.A., Bothmes, V., 2003. Identification of solar sources of major geomagnetic storms between 1996 and 2000. Astrophys. J. 582, 520.